SAND2023-04781C

Sandia National Laboratories

Anoxic Iron Corrosion Characterization in the Waste Isolation Pilot Plant

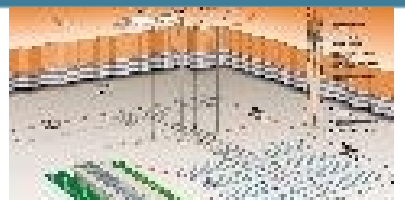

Ania Pavitt

ABC–Salt (VII) Workshop, 15-16 June 2023, Santa Fe, NM-USA

Sandia National Laboratories is a multimission laboratory managed and operated by National Technology & Engineering Solutions of Sandia, LLC, a wholly owned subsidiary of Honeywell International Inc., for the U.S. Department of Energy's National Nuclear Security Administration under contract DE-NA0003525. This research is funded by WIPP programs administered by the Office of Environmental Management (EM) of the U.S. Department of Energy.

Sandia National Laboratories is a multimission laboratory managed and operated by National Technology & Engineering Solutions of Sandia, LLC, a wholly owned subsidiary of Honeywell International Inc., for the U.S. Department of Energy's National Nuclear Security Administration under contract DE-NA0003525.

Overview

1. Importance of corrosion work at the WIPP
2. Past experiments conducted at Sandia National Laboratories
   - Details
   - Conclusion/ Results
3. Current methods to study rates and products of anoxic iron corrosion
   - Details
   - Expected results

Gamry, Bruker, Hitachi

1. Importance of corrosion work at the WIPP

- Uncertainty in the process model with respect to iron (Fe) corrosion
  - Rates
  - Products
- Predicted that corrosion is the main contributor of gas generated in the repository
- Main corrosion products are expected to be ferrous hydroxide ($Fe(OH)_2$) and magnetite (Fe_3O_4)

1. $Fe(s) + 2\ H_2O(l) \rightarrow Fe(OH)_2(s) + H_2(g)$
2. $3\ Fe(s) + 4\ H_2O(l) \rightarrow Fe_3O_4(s) + 4\ H_2(g)$

t > x days:

3. $3\ Fe(OH)_2(s) \rightarrow Fe_3O_4(s) + 2\ H_2O(l) + H_2(g)$

- Important to know which reaction will dominate
- Reaction (2) will cause a pressure build up above lithostatic pressure of the repository (~150 atm)
  - This scenario could help transport radionuclides to the surface
- Other mechanisms of radionuclide release include change in redox state which will affect its mobility

2. Past experiments conducted at Sandia National Laboratories

1985-2019

2.1 WIPP Materials Interface Interactions Test (Molecke, Sorensen, and Wicks 1986-1991)

- Methods
  - Mass loss
  - Microscopy (low and high powered)
  - Knoop microhardness
- Details
  - 6, 12, 24, 60 month sampling, T = 90˚C
  - Almost 2000 samples buried in the WIPP in 50 separate test assemblies (shown)
  - Participation from 7 countries
    - Samples
    - Post-test analysis
    - Participation in Peer Review

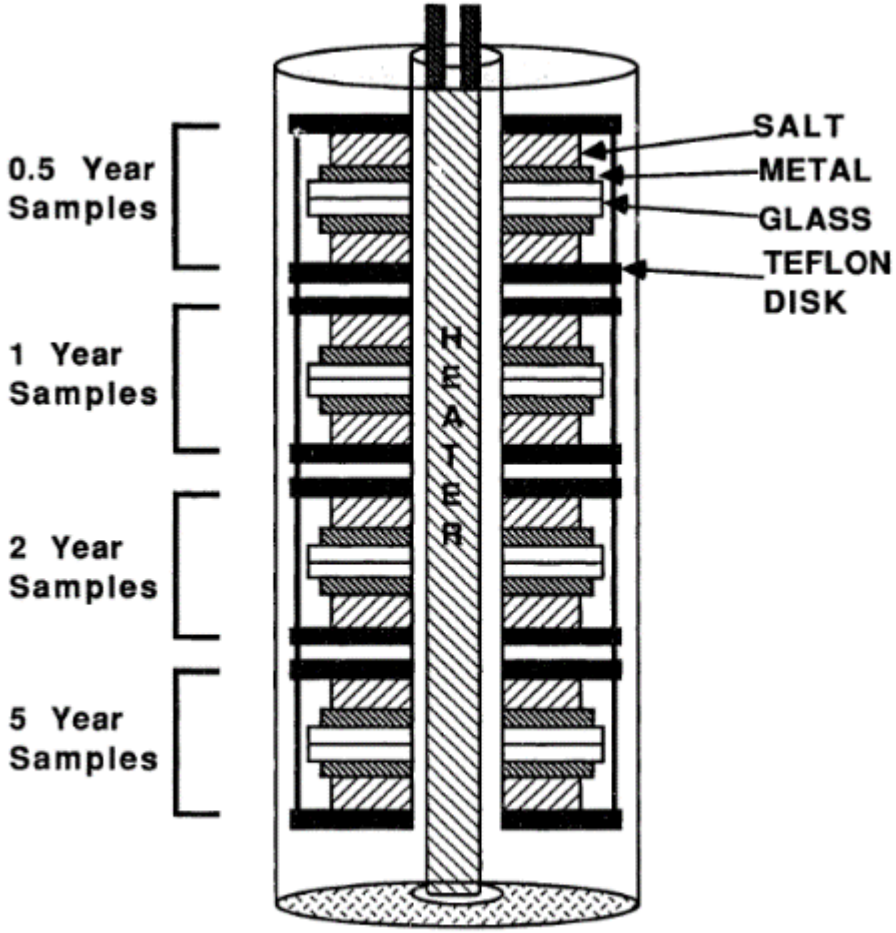

Figure 1-15. WIPP MIIT sample assembly.

(Molecke, Sorensen et al. 1993)

2.1 Molecke, Sorensen, and Wicks Results

- Corrosion was localized (not general) therefore rates could not be calculated using mass loss
- Data were presented as changes in weight
- Change in weight for carbon steel (shown)
- Localized (pitting, crevice, stress)
  - Austenitic steel
- General
  - Lead
- Localized and general
  - Mild steels, copper

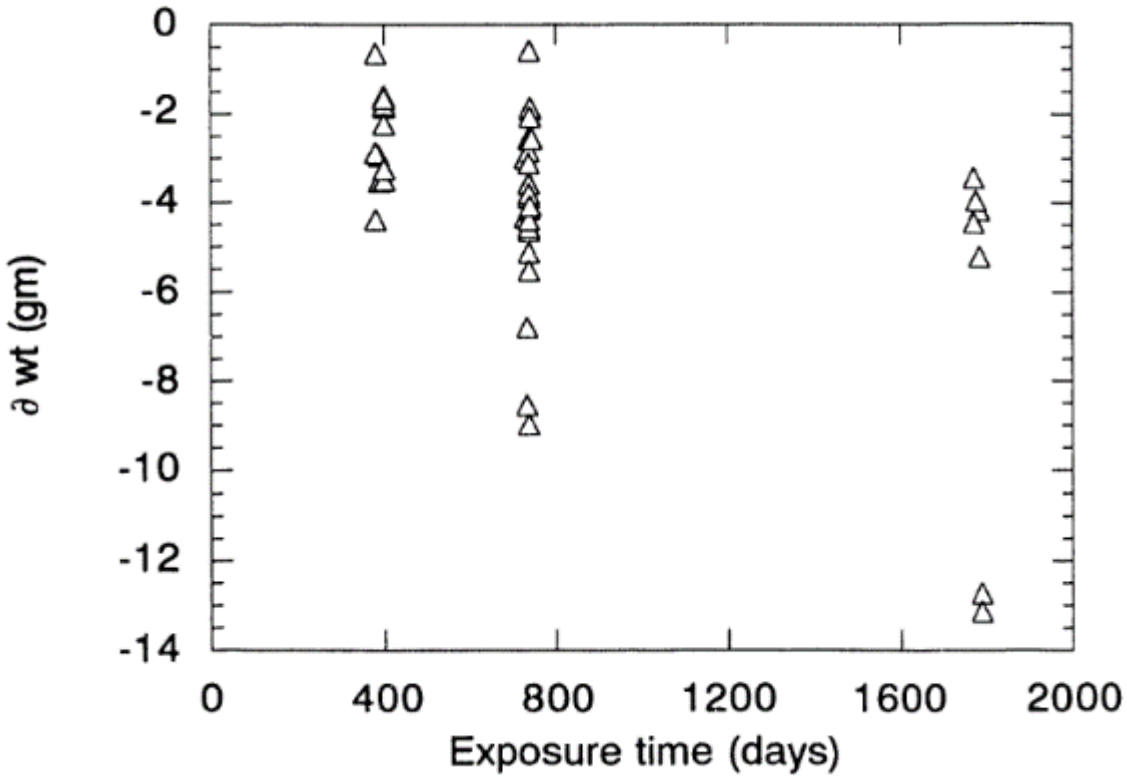

(Molecke, Sorensen et al. 1993)

2.2 Hydrogen Generation by Metal Corrosion in Simulated WIPP Environments (Telander and Westerman 1989-1995)

- Methods
  - Mass loss
  - H_2 pressure (seal welded (P < 20 atm and autoclave (P > 20 atm))
  - X-ray powder diffraction (XRD)
  - Inductively coupled plasma - optical emission spectroscopy (ICP-OES)
- Details
  - pH 3-11, T = 30˚C, t = 3-38 months
  - Four material types (low carbon steel, Ti, Cu, Al based materials)
  - Brine with overpressures (N_2, CO_2, H_2S, H_2)
  - Samples fully immersed or vapor phase
  - Correlation between H_2 pressure, corrosion rate and corrosion products

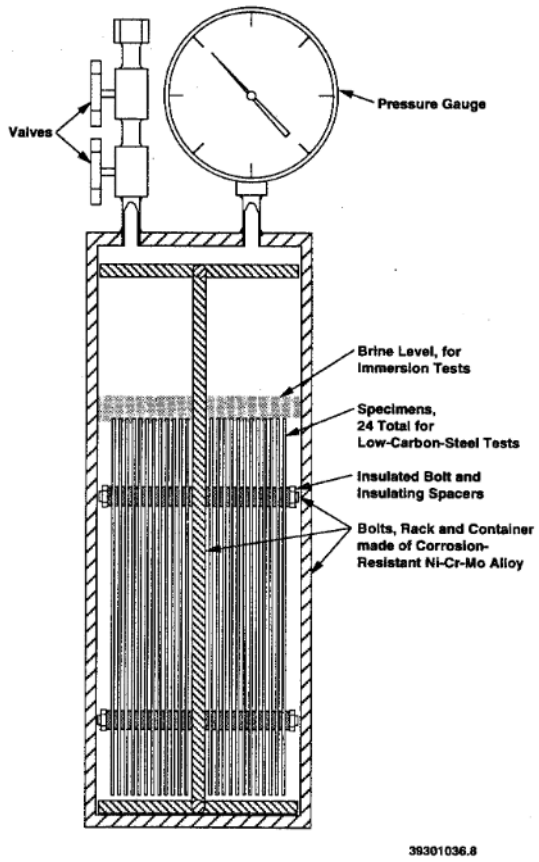

Figure 5-1. Seal-welded test container with specimen rack in place. Inside dimensions (typical): 28.9 cm (11.4 in.) high, 10.2 cm (4.0 in.) diameter.

(Telander and Westerman 1997)

2.2 Telander and Westerman Results

- Average corrosion rates of low carbon steel (6 months, brine A (Salado)) at various overpressures
- N_2 µm/yr (atm)
  - 1.72 (10), 2.97 (73), 2.72 (127)
- H_2
  - 1.72 (2), 0.36 (70), 1.02 (127)
- CO_2
  - 6.30 (10) , 29.7 (36), 33.6 (62)
- H_2S
  - No significant reaction (5)

- Corrosion products (XRD) at various over pressures
- N_2
  - Unidentifiable with XRD (ICP, Fe with 12% Mg)
- H_2
  - Reevesite (nickel iron carbonate hydroxide, possibly from autoclave (Ni-Cr-Mo alloys))
- CO_2
  - Oligonite $(FeMnZn)CO_3$
- H_2S
  - Mackinawite (FeS)

(Telander and Westerman 1997)

2.3 Iron and Lead Corrosion in WIPP Relevant Conditions: 6, 12, 18, 24 Months Result (Roselle 2009-2013)

- Methods
  - Mass loss
  - Scanning electron microscopy/energy dispersive X-ray spectroscopy (SEM/EDS)
- Details
  - 6, 12, 18, 24 months sampling
  - Steel and lead coupons suspended, immersed, or partially immersed for 2 years
  - 4 brines (equilibrated with MgO)
    - Generic weep brine (GWB) (w and w/o organics)
    - ERDA-6 (w and w/o organics)
  - Atmosphere 0-3500 ppm CO_2
  - T = 26˚C

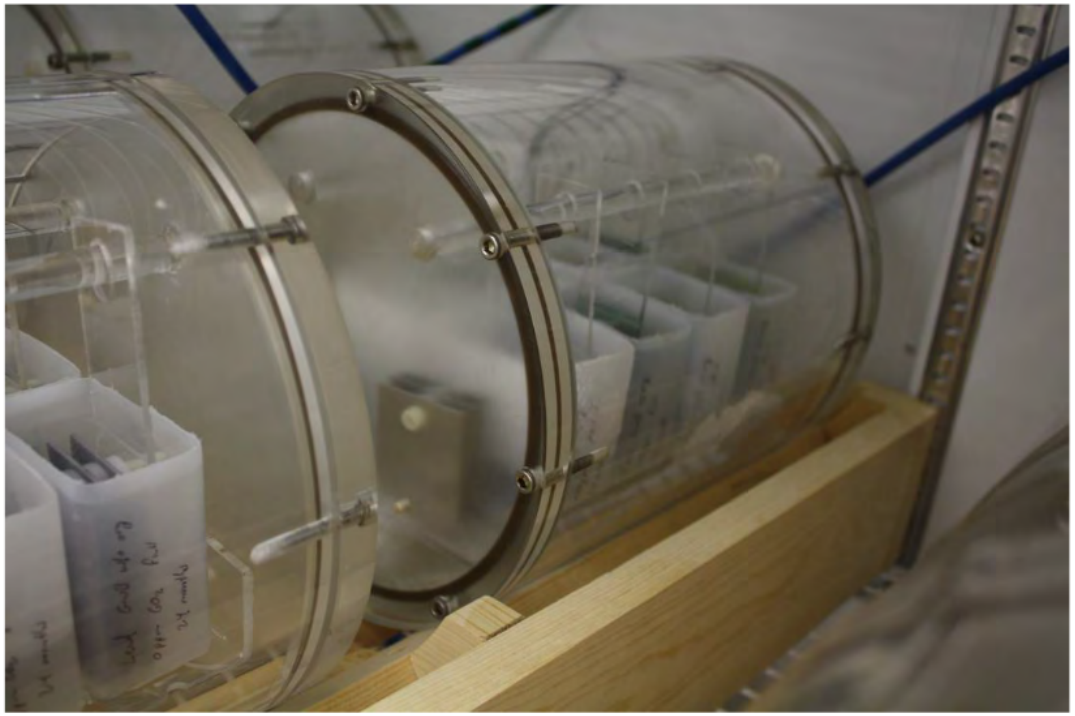

Figure 3-3 Specimen test Chambers inside the Incubator

(Roselle 2009)

2.3 Roselle Results

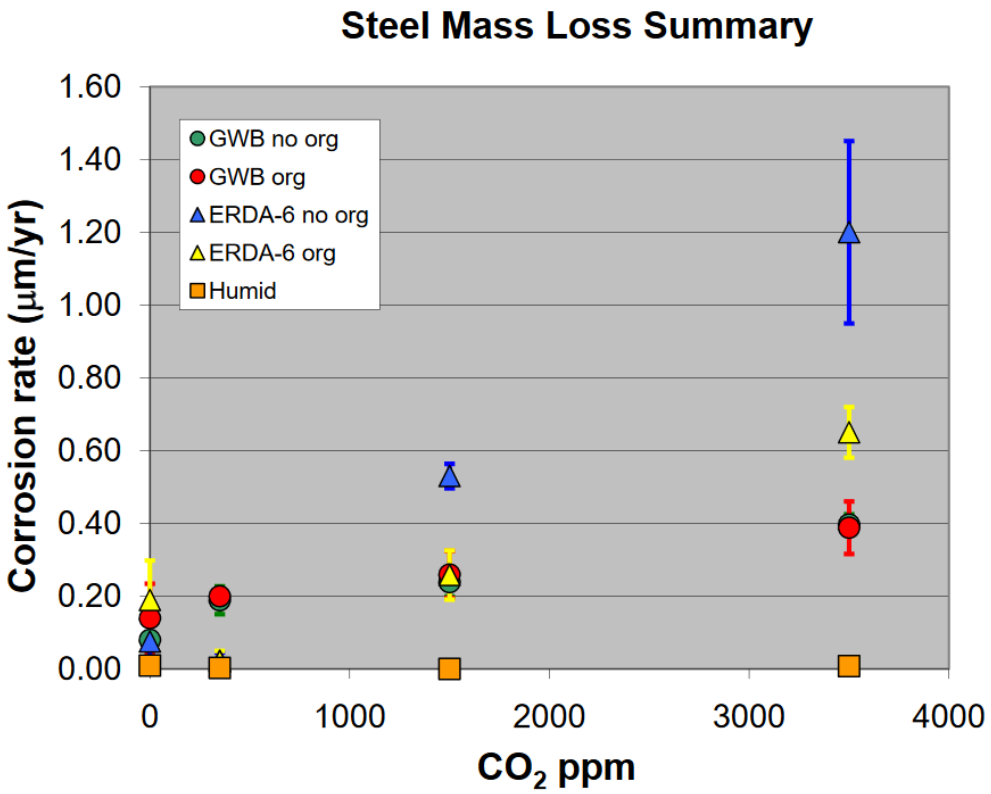

Figure 4-28 Average corrosion rates for steel coupons in the various brines plotted as a function of the atmospheric CO_2 concentration. Bars indicate one standard deviation for the average corrosion rates.

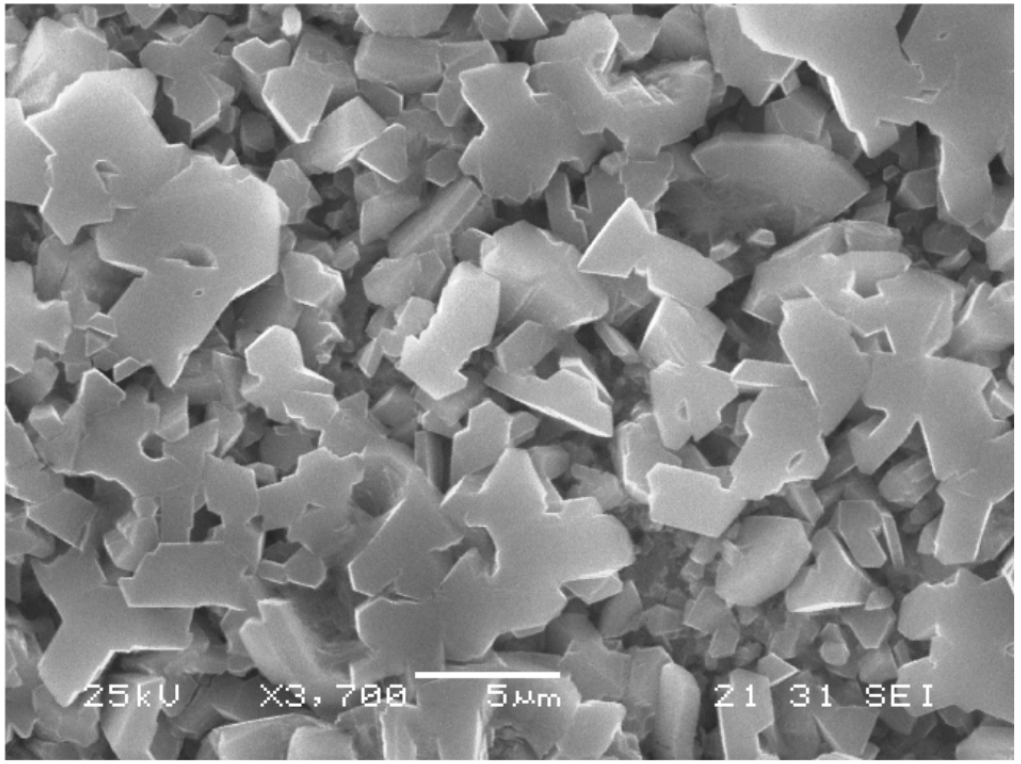

Figure 4-10 SEM image of corrosion product "iron chloride 1" formed on partially submerged coupon 104. This phase forms the green band on partially submerged samples at the brine/atmosphere interface in all brine types and CO_2 concentrations. Image source: *104E_2.BMP* located on disk in "WIPP-FePb-3 Supplemental Binder D".

(Roselle 2009)

2.4 Iron and Lead Corrosion in WIPP Relevant Conditions (Sisk-Scott and Icenhower 2015-2019)

- Methods
  - Mass loss
  - Interferometry
  - Release of Fe into solution ICP-OES, MS
  - H_2 release pressure gauge, gas chromatography – thermal conductivity detector (GC-TCD)
  - XRD
  - Raman spectroscopy
  - SEM/EDS
- Details
  - 6 months, glovebox, T = 90˚C
  - Steel (Alabama Specialty Products)
  - Single pass flow through (60 mL/day)
  - 3.5 M NaCl and 1 M $MgCl_2$ brine (simplified GWB) w and w/o NaHS

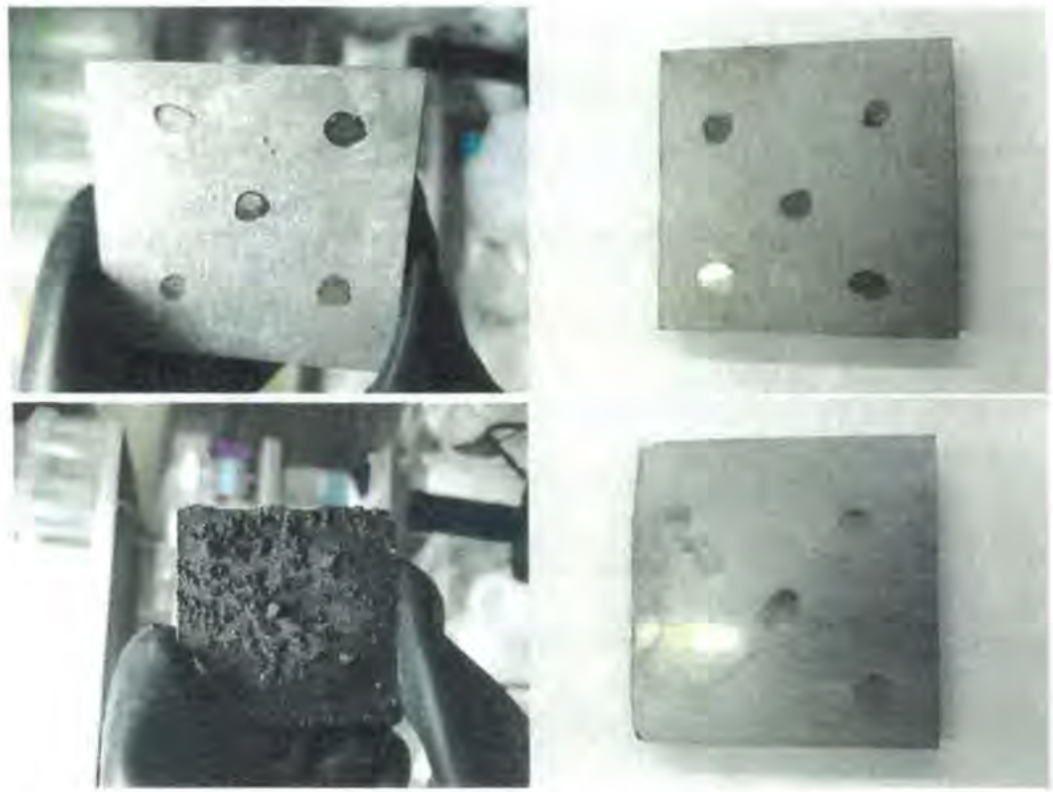

Figure 24. Photographs of post-experiment steel coupons. A. Coupon 113 (SGWB) before cleaning. B. Coupon 113 after cleaning. C. Coupon D (SGWB + NaHS) before cleaning. D. Coupon D after cleaning.

(Sisk-Scott 2019)

2.4 Sisk-Scott and Icenhower Results

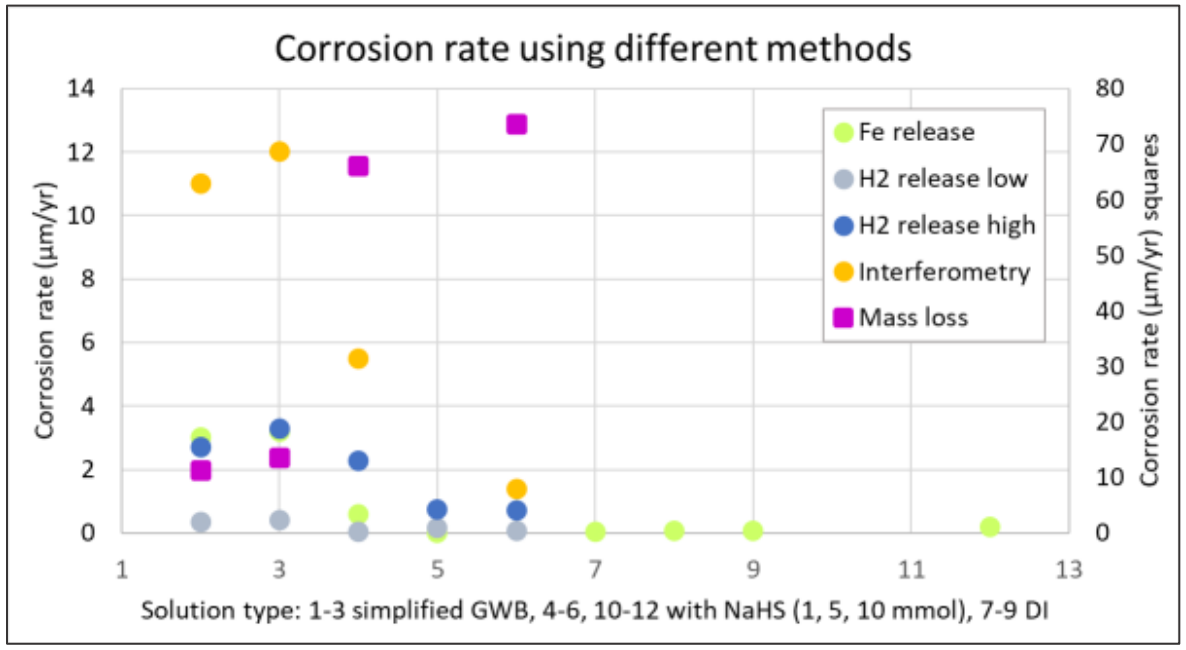

- Corrosion products using XRD and Raman
  - XRD - iron chloride hydroxide and akageneite (possibly from air exposure) XRD
  - Raman - magnetite, mackinawite

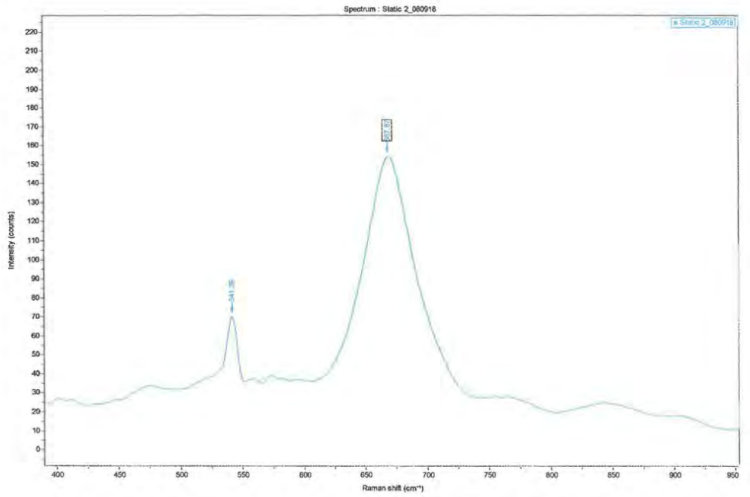

Figure 15. Raman spectrum of magnetite detected on Coupon 2 from static experiments in simplified GWB brine (λ=638 nm).

(Sisk-Scott 2019)

2.5 Iron and Lead Corrosion in WIPP Relevant Conditions (Zhang 2019)

- Methods
  - Mass loss
  - Interferometry
  - ICP-MS (Fe release)
  - Electrochemistry (electrochemical impedance spectroscopy, potentiodynamic polarization
  - XRD
  - SEM/EDS
- Details
  - 6 months, glovebox, T = 90˚C
  - 180 mL Teflon reactors sampled weekly
  - Simplified GWB
  - Single pass flow through (60 mL/day)
  - Steel (C1018)

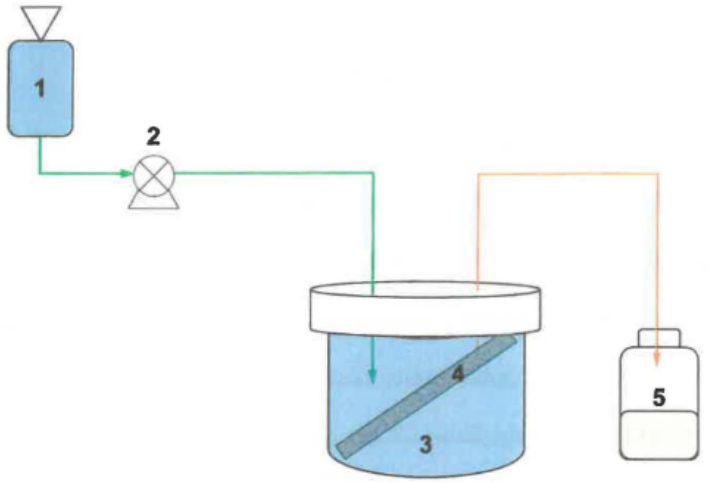

Figure 1. Flow diagram of a SPFT reactor. It consists of Brine reservoir (1), Peristaltic pump (2), 180 mL Sealed Teflon vessel (3), Steel coupon (4), and Effluent collection container (5).

(Zhang 2020)

2.5 Zhang 2019 Results

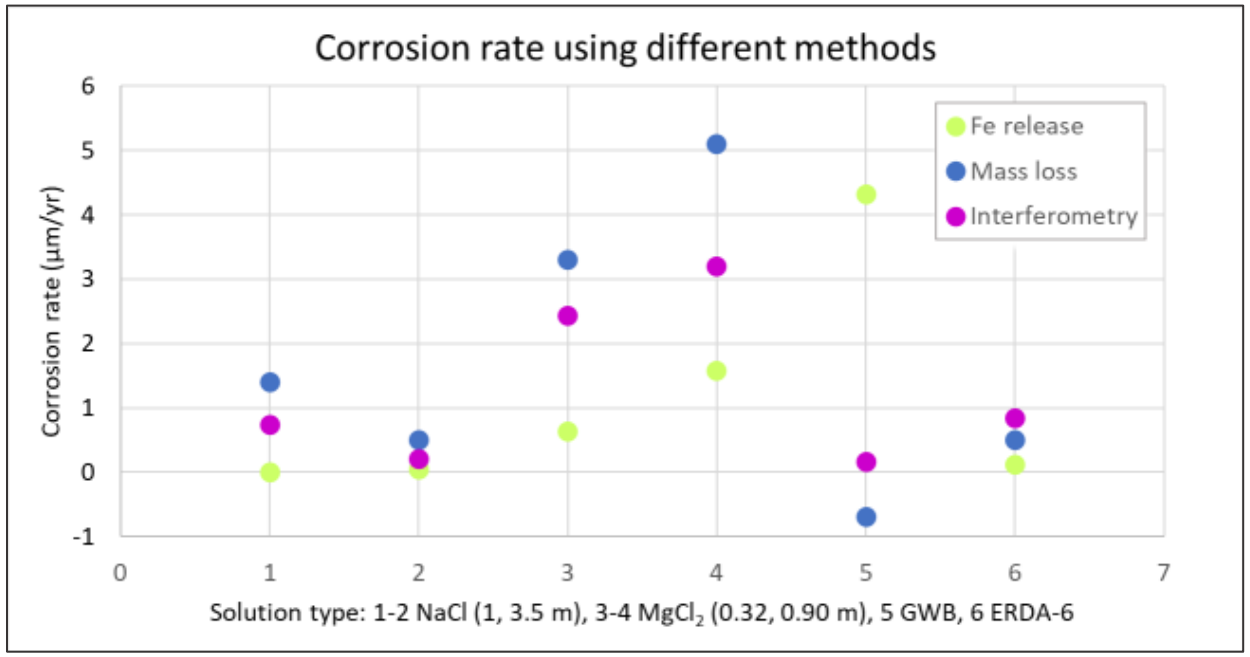

- Corrosion products
  - Not enough sample for XRD analysis
  - SEM/EDS Fe and Cl (shown)

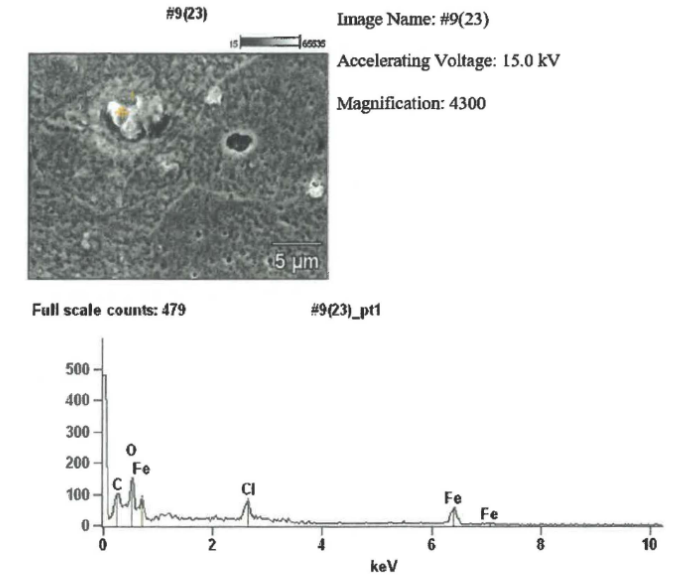

Figure 29. SEM Image the Fe coupon surface from the 6-month SPFT experiment in GWB at 90 °C and EDS analyses of solid particles on the surface at different spots.

(Zhang 2020)

3. Current methods to study rates and products of anoxic iron corrosion

2023

3.1 Iron Corrosion Characterization Under Atmospheric and High-Pressure Conditions (Pavitt 2023)

- Methods
  - Mass loss combined with in situ measurements (E_{CORR}, pH, Fe(II))
  - UV-Vis
  - Raman Spectroscopy
  - SEM/EDS
- Details
  - Glovebox, T = 27˚C, pH 8.8
  - Four electrochemical (EC) cells per brine (GWB, ERDA-6, NaCl)
  - Three samples (electrodes) per EC cell
    - Two corroding (Fe coupons)
    - One non-corroding (glassy carbon)
  - Three-part experiment
    - Atmospheric pressure (A, B)
    - High pressure

Corr Instruments, Pine Research

3.2 Iron corrosion at pressures = 0.1 MPa

Experiment 1A – Mass loss in glass electrochemical cell

- Measure during mass loss
  - E_{CORR}
  - pH
  - $Fe(II)_{aq}$
  - Temperature
  - Electrochemical frequency modulation (rate)
  - UV-Vis (products)
  - Raman (products)
- Post mass loss
  - UV-Vis (products)
  - Raman (products)
  - SEM/EDS (products)

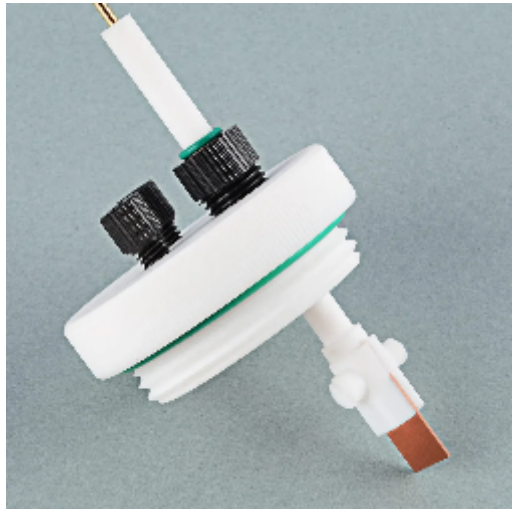

Pine Research, StonyLab

3.3 Iron corrosion at pressures = 0.1 MPa

Experiment 1B – Mass loss in sealed reactor

- Measure during mass loss
  - E_{CORR}
  - pH
  - Temperature
  - Electrochemical frequency modulation (rate)
  - H_2 evolution (rate)
- Post mass loss
  - UV-Vis (products)
  - Raman (products)
  - SEM/EDS (products)

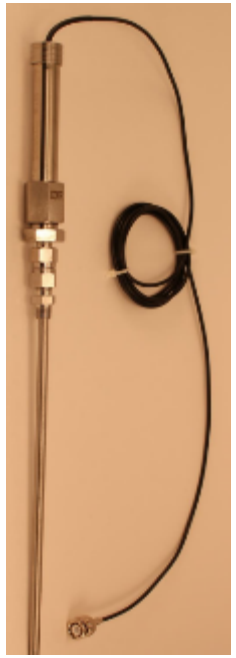

Parr Instruments, Corr instruments

3.4 Iron corrosion at pressures 0.1 - 15 MPa

Experiment 2 – Mass loss in pressurized electrochemical cell

- Measure during mass loss
  - E_{corr}
  - pH
  - Temperature
  - Electrochemical frequency modulation (rate)
- Post mass loss
  - UV-Vis (products)
  - Raman (products)
  - SEM/EDS (products)

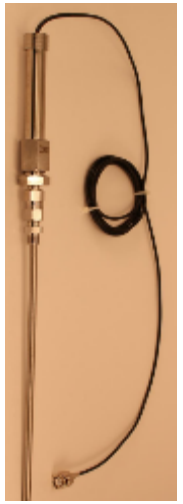

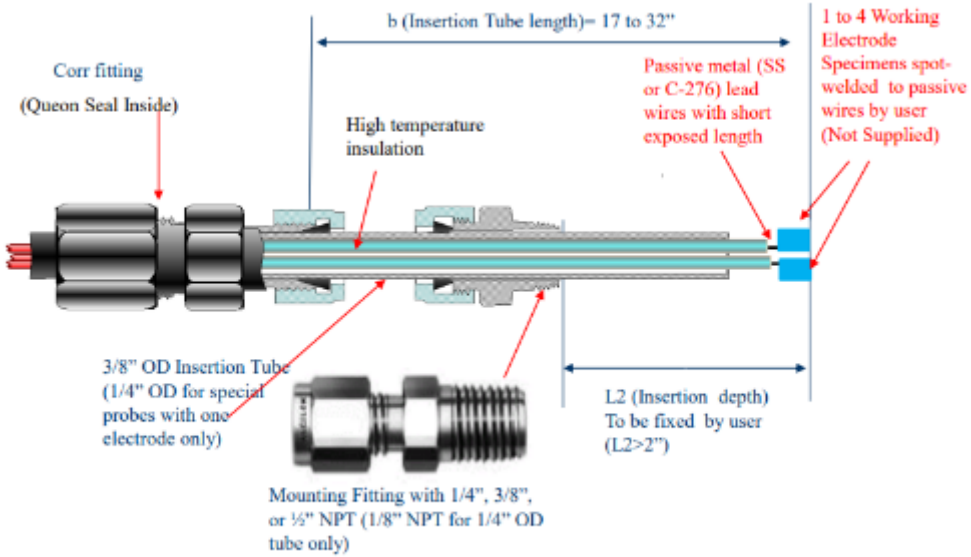

3.5 Expected Results

- E_{CORR}/ pH data can be used to construct Pourbaix diagrams that can aid in predicting corrosion products
- Other corrosion product characterization methods shown
  - Raman
  - UV-Vis

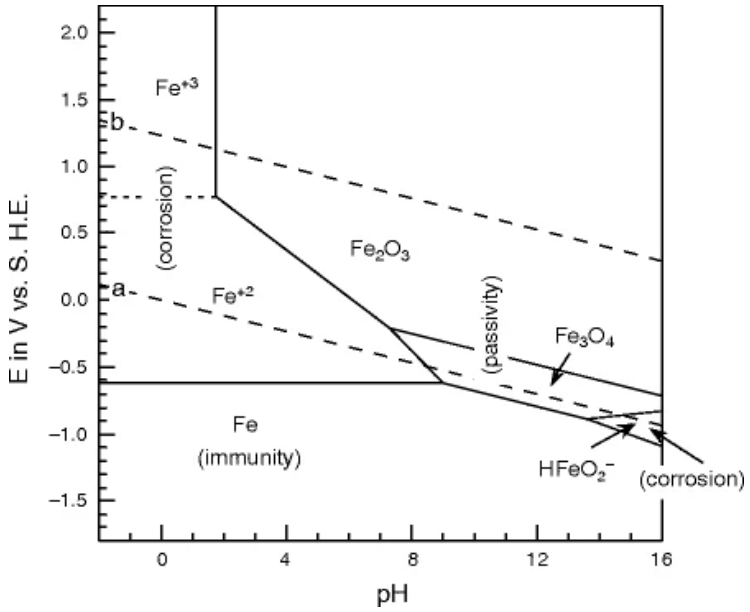

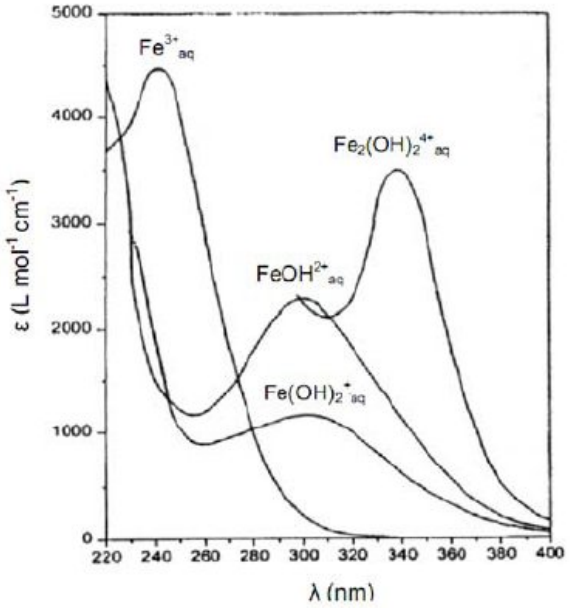

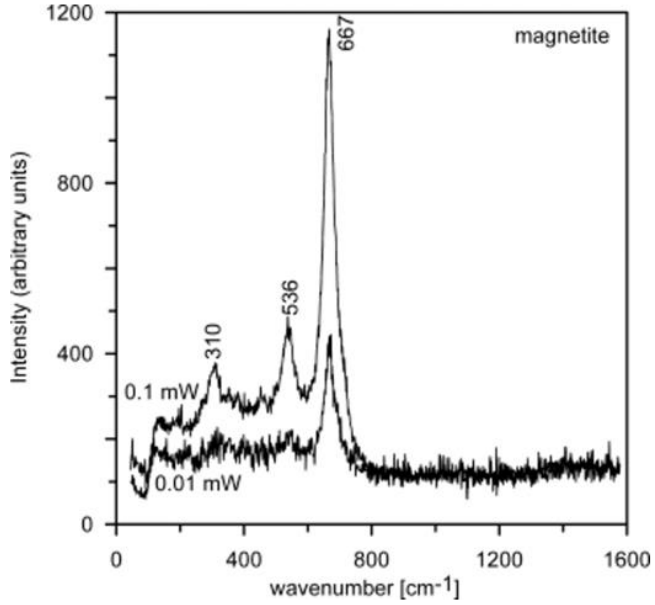

(McCafferty 2010, Loures, Alcântara et al. 2013, Hanesch 2009)

References

- Molecke, M. A., et al. 1993. Waste Isolation Pilot Plant Materials Interface Interactions Test: Papers presented at the Commission of European Communities workshop on in situ testing of radioactive waste forms and engineered barriers. United States.
- Telander, M. R. and R. E. Westerman. 1997. Hydrogen generation by metal corrosion in simulated Waste Isolation Pilot Plant environments. Albuquerque, NM. SAND96-2538
- Roselle, G. T. 2009. Iron and Lead Corrosion in WIPP-Relevant Conditions: Six Month Results [Milestone Report]. Carlsbad, NM. ERMS 552218
- Sisk-Scott, C. 2019. Milestone Report for Iron and Lead Corrosion in WIPP-Relevant Conditions: Static and Solution Flow-Through Corrosion Experiments. Carlsbad, NM.
- Zhang, L. 2020. FY20 Milestone Report on TP 06-02 Rev. 3. Carlsbad, NM.
- McCafferty, E. (2010). Thermodynamics of Corrosion: Pourbaix Diagrams. Introduction to Corrosion Science. E. McCafferty. New York, NY, Springer New York: 95-117.
- Loures, C. C. A., et al. (2013). Advanced Oxidative Degradation Processes: Fundamentals and Applications.
- Hanesch, M. 2009. Raman spectroscopy of iron oxides and (oxy)hydroxides at low laser power and possible applications in environmental magnetic studies. *Geophysical Journal International*, *177*(3), 941-948.

Questions?